Supplement of Atmos. Chem. Phys., 23, 7103–7120, 2023
https://doi.org/10.5194/acp-23-7103-2023-supplement

Atmospheric Chemistry and Physics Open Access

Supplement of

Photoaging of phenolic secondary organic aerosol in the aqueous phase: evolution of chemical and optical properties and effects of oxidants

Wenqing Jiang et al.

Correspondence to: Qi Zhang (dkwzhang@ucdavis.edu)

Table of Contents

S1. Calculation of the light absorption properties of the aqSOA

The light absorption coefficient (α_{λ}, cm^{-1}) of the aqSOA was calculated as:

$$\alpha_{\lambda} = \frac{A_{total,\lambda} - A_{GA,\lambda} - A_{DMB,\lambda}}{l} \quad \text{(Eq. S1)}$$

where $A_{total,\lambda}$ is the total measured base-10 light absorbance of the solution at wavelength λ, $A_{GA,\lambda}$ and $A_{DMB,\lambda}$ denote the absorbance contributed by GA and 3,4-DMB, and l is the pathlength of the cuvette (1 cm). The mass absorption coefficient (MAC_{λ}, $m^2\ g^{-1}$) of the aqSOA was calculated as:

$$MAC_{\lambda} = \frac{2.303 \times \alpha_{\lambda}}{[Org]_{solution}} \times 100 \quad \text{(Eq. S2)}$$

where $[Org]_{solution}$ is the aqSOA mass concentration (μg mL^{-1}) in the solution, 2.303 is a conversion factor between log10 and natural log, and 100 is for unit conversion. The absorption Ångström exponent (AAE) of the aqSOA was calculated as:

$$AAE_{\lambda 1-\lambda 2} = -\frac{\ln\frac{\alpha_{\lambda 1}}{\alpha_{\lambda 2}}}{\ln\frac{\lambda 1}{\lambda 2}} \quad \text{(Eq. S3)}$$

where $\alpha_{\lambda 1}$ and $\alpha_{\lambda 2}$ denote the light absorption coefficients at wavelengths λ_1 and λ_2. The rate of sunlight absorption of the aqSOA (R_{abs}, mol photons $L^{-1}\ s^{-1}$) was calculated as:

$$R_{abs} = 2.303 \times \frac{10^3}{N_A} \times \sum_{290\ nm}^{500\ nm}(\alpha_{\lambda} \times I_{\lambda} \times \Delta\lambda) \quad \text{(Eq. S4)}$$

where I_{λ} is the midday winter-solstice actinic flux in Davis (photons $cm^{-2}\ s^{-1}\ nm^{-1}$) from the Tropospheric Ultraviolet and Visible (TUV) Radiation Model version 5.3 (https://www.acom.ucar.edu/Models/TUV/Interactive_TUV/), Δλ is the interval between adjacent wavelengths in the TUV output, 2.303 is for base conversion between log10 and natural log, 10^3 is for unit conversion, and N_A is Avogadro's number.

Table S1. The •OH-aqSOA mass yield, H/C, O/C and OS_C determined by HR-ToF-AMS during aqSOA formation and aging.

	Irradiation Time (h)	SOA yield	H/C	O/C	OSc
•OH-aqSOA formation	0.5	9.72E-01	1.64	0.32	-1.00
	1	8.60E-01	1.52	0.43	-0.66
	2	1.03E+00	1.46	0.51	-0.45
	3	1.06E+00	1.43	0.54	-0.34
	4	9.24E-01	1.43	0.55	-0.33
	6	8.16E-01	1.42	0.57	-0.27
	8	7.39E-01	1.41	0.60	-0.21
	10	6.70E-01	1.41	0.60	-0.21
	12	5.93E-01	1.39	0.62	-0.15
	24	4.60E-01	1.38	0.65	-0.10
•OH-aqSOA aging (no addition of extra oxidant)	25	4.41E-01	1.38	0.66	-0.06
	26	4.31E-01	1.37	0.66	-0.06
	28	4.16E-01	1.37	0.66	-0.06
	30	3.96E-01	1.37	0.67	-0.03
	35	3.55E-01	1.36	0.67	-0.02
	36	3.50E-01	1.36	0.67	-0.02
	40	3.26E-01	1.36	0.67	-0.02
	44	3.05E-01	1.36	0.67	-0.01
	48	2.82E-01	1.36	0.67	-0.02
	60	2.34E-01	1.35	0.67	-0.01
	70	2.07E-01	1.36	0.67	-0.01
	72	2.02E-01	1.35	0.68	0.02
•OH-aqSOA aging (add 100 μM of H2O2)	25	4.54E-01	1.39	0.68	-0.03
	26	4.48E-01	1.39	0.70	0.01
	28	3.74E-01	1.39	0.70	0.01
	30	3.10E-01	1.39	0.70	0.01
	35	1.96E-01	1.40	0.68	-0.04
	36	1.85E-01	1.41	0.66	-0.08
	40	1.56E-01	1.41	0.64	-0.13
	44	1.21E-01	1.40	0.64	-0.12
	48	9.55E-02	1.40	0.64	-0.12
	60	7.43E-02	1.43	0.61	-0.21
	70	6.39E-02	1.44	0.57	-0.29
	72	6.14E-02	1.44	0.57	-0.29
•OH-aqSOA aging (add 5 μM of 3,4-DMB)	25	4.88E-01	1.38	0.66	-0.05
	26	4.48E-01	1.38	0.67	-0.04
	28	4.20E-01	1.37	0.69	0.01
	30	3.99E-01	1.39	0.68	-0.03
	35	2.99E-01	1.40	0.67	-0.05
	36	2.85E-01	1.40	0.67	-0.05
	40	2.40E-01	1.40	0.66	-0.08
	44	2.14E-01	1.41	0.66	-0.09
	48	1.89E-01	1.41	0.65	-0.10
	60	1.37E-01	1.41	0.64	-0.12
	70	1.13E-01	1.42	0.62	-0.17
	72	1.10E-01	1.43	0.61	-0.20
•OH-aqSOA aging (dark)	24	4.29E-01	1.39	0.65	-0.09
	48	4.31E-01	1.39	0.66	-0.07
	72	4.43E-01	1.37	0.66	-0.05

Table S2. The ^{3}C*-aqSOA mass yield, H/C, O/C and OS_C determined by HR-ToF-AMS during aqSOA formation and aging.

	Irradiation Time (h)	SOA yield	H/C	O/C	OSc
^{3}C*-aqSOA formation	0.3	/	1.61	0.37	-0.88
	0.6	9.03E-01	1.53	0.43	-0.67
	0.9	8.90E-01	1.50	0.46	-0.58
	1.2	8.83E-01	1.49	0.48	-0.52
	1.7	8.69E-01	1.48	0.51	-0.46
	2.3	8.58E-01	1.47	0.54	-0.39
	2.9	8.50E-01	1.46	0.54	-0.38
	3.5	8.58E-01	1.44	0.58	-0.29
^{3}C*-aqSOA aging (no addition of extra oxidant)	3.8	8.39E-01	1.43	0.60	-0.23
	4.1	8.52E-01	1.43	0.62	-0.17
	4.3	8.45E-01	1.42	0.64	-0.15
	4.6	8.23E-01	1.43	0.65	-0.13
	4.9	8.13E-01	1.43	0.64	-0.15
	5.2	8.02E-01	1.42	0.68	-0.06
	5.8	7.80E-01	1.42	0.71	-0.01
	6.4	7.49E-01	1.42	0.73	0.03
	7.0	7.16E-01	1.42	0.74	0.05
	8.1	6.33E-01	1.43	0.75	0.06
	9.3	5.76E-01	1.43	0.76	0.10
	11.6	5.05E-01	1.43	0.77	0.11
	13.9	4.43E-01	1.43	0.77	0.12
^{3}C*-aqSOA aging (add 100 μM of H2O2)	3.8	8.44E-01	1.44	0.59	-0.24
	4.1	8.42E-01	1.43	0.62	-0.17
	4.3	8.33E-01	1.42	0.65	-0.12
	4.6	8.04E-01	1.43	0.68	-0.06
	4.9	7.95E-01	1.42	0.70	-0.02
	5.2	7.83E-01	1.42	0.70	-0.01
	5.8	7.52E-01	1.41	0.72	0.03
	6.4	7.14E-01	1.41	0.73	0.05
	7.0	6.85E-01	1.42	0.74	0.07
	8.1	6.30E-01	1.42	0.75	0.08
	9.3	5.70E-01	1.43	0.76	0.10
	11.6	4.89E-01	1.45	0.74	0.02
	13.9	3.81E-01	1.45	0.76	0.07
^{3}C*-aqSOA aging (add 5 μM of 3,4-DMB)	3.8	8.48E-01	1.42	0.58	-0.30
	4.1	8.44E-01	1.42	0.59	-0.28
	4.3	8.50E-01	1.42	0.59	-0.26
	4.6	8.46E-01	1.42	0.59	-0.22
	4.9	8.41E-01	1.43	0.61	-0.19
	5.2	8.41E-01	1.43	0.61	-0.18
	5.8	8.31E-01	1.41	0.63	-0.15
	6.4	8.22E-01	1.42	0.65	-0.12
	7.0	8.08E-01	1.42	0.66	-0.09
	8.1	7.73E-01	1.42	0.68	-0.07
	9.3	7.45E-01	1.42	0.69	-0.04
	11.6	6.82E-01	1.43	0.70	-0.02
	13.9	6.38E-01	1.43	0.71	-0.02
^{3}C*-aqSOA aging (dark)	7.0	9.05E-01	1.44	0.59	-0.26
	13.9	9.25E-01	1.43	0.60	-0.24

65

Table S3. Exponential fits for aqSOA formation and decay.

	Pseudo-first-order decay of GA	Exponential fit for initial aqSOA formation	Exponential fit for aqSOA decay	
•OH-aqSOA	$[GA]_t/[GA]_0 = e^{-0.144t}$	$y = 14.8(1-e^{-0.167x})$	No addition of extra oxidant:	$y = 7.4e^{-0.017x}$
			Add 100 μM of H_2O_2:	$y = 6.6e^{-0.11x}+1.08$
			Add 5 μM of 3,4-DMB:	$y = 6.3e^{-0.057x}+1.44$
$^3C^*$-aqSOA	$[GA]_t/[GA]_0 = e^{-0.727t}$	$y = 14.5(1-e^{-0.945x})$	No addition of extra oxidant:	$y = 15.1e^{-0.073x}$
			Add 100 μM of H_2O_2:	$y = 15.3e^{-0.078x}$
			Add 5 μM of 3,4-DMB:	$y = 15.7e^{-0.034x}$

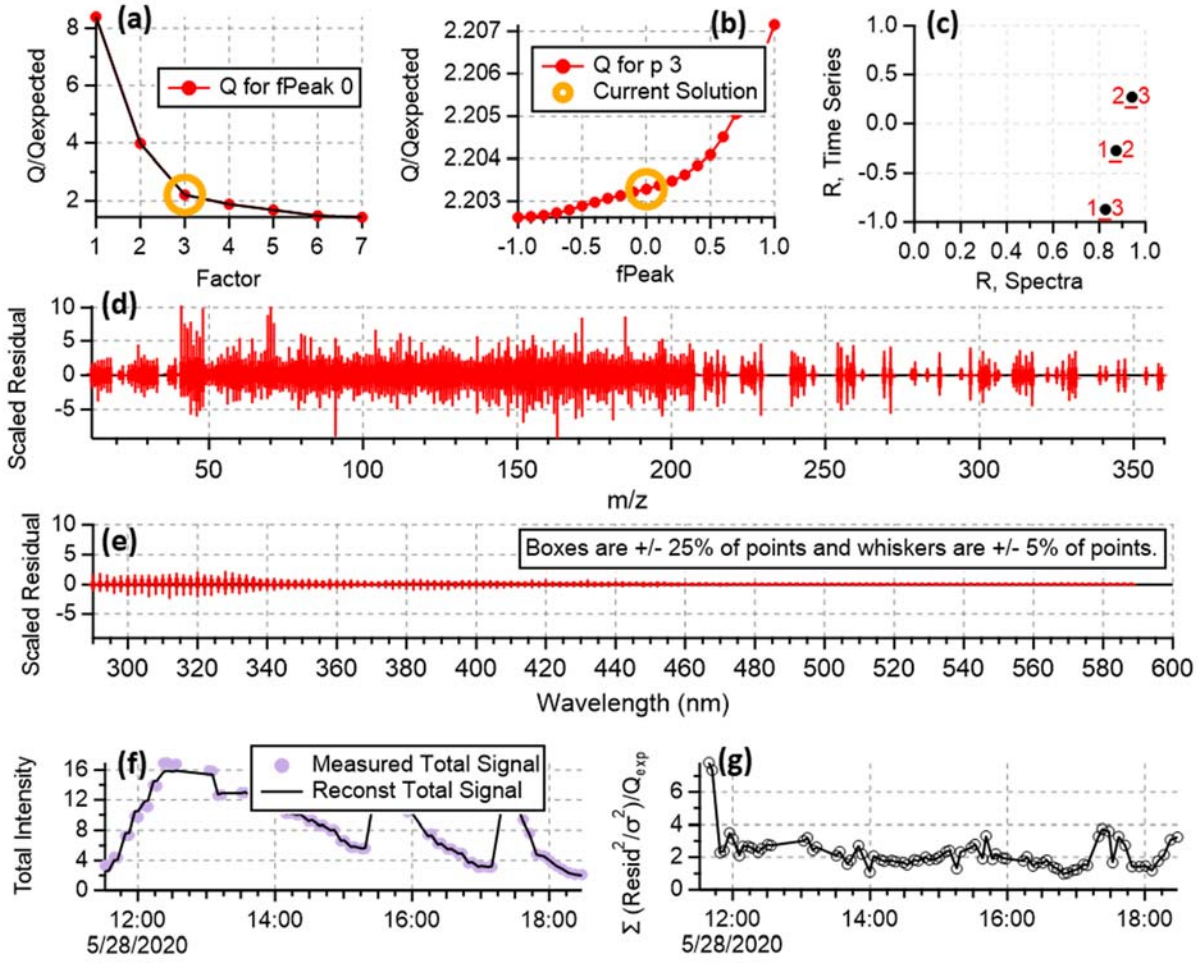

Figure S1. Summary of diagnostic plots of the PMF analysis of the •OH-initiated reactions : (a) Q/Q_{exp} as a function of number of factors selected for PMF modeling. (b) Q/Q_{exp} as a function of fPeak. (c) Correlations among PMF factors. (d) Box and whisker plot showing the distributions of scaled residuals for each AMS ion. (e) Box and whisker plot showing the distributions of scaled residuals for each light absorption wavelength. (f) Reconstructed and measured total signal for each sample. (g) Q/Q_{exp} for each sample.

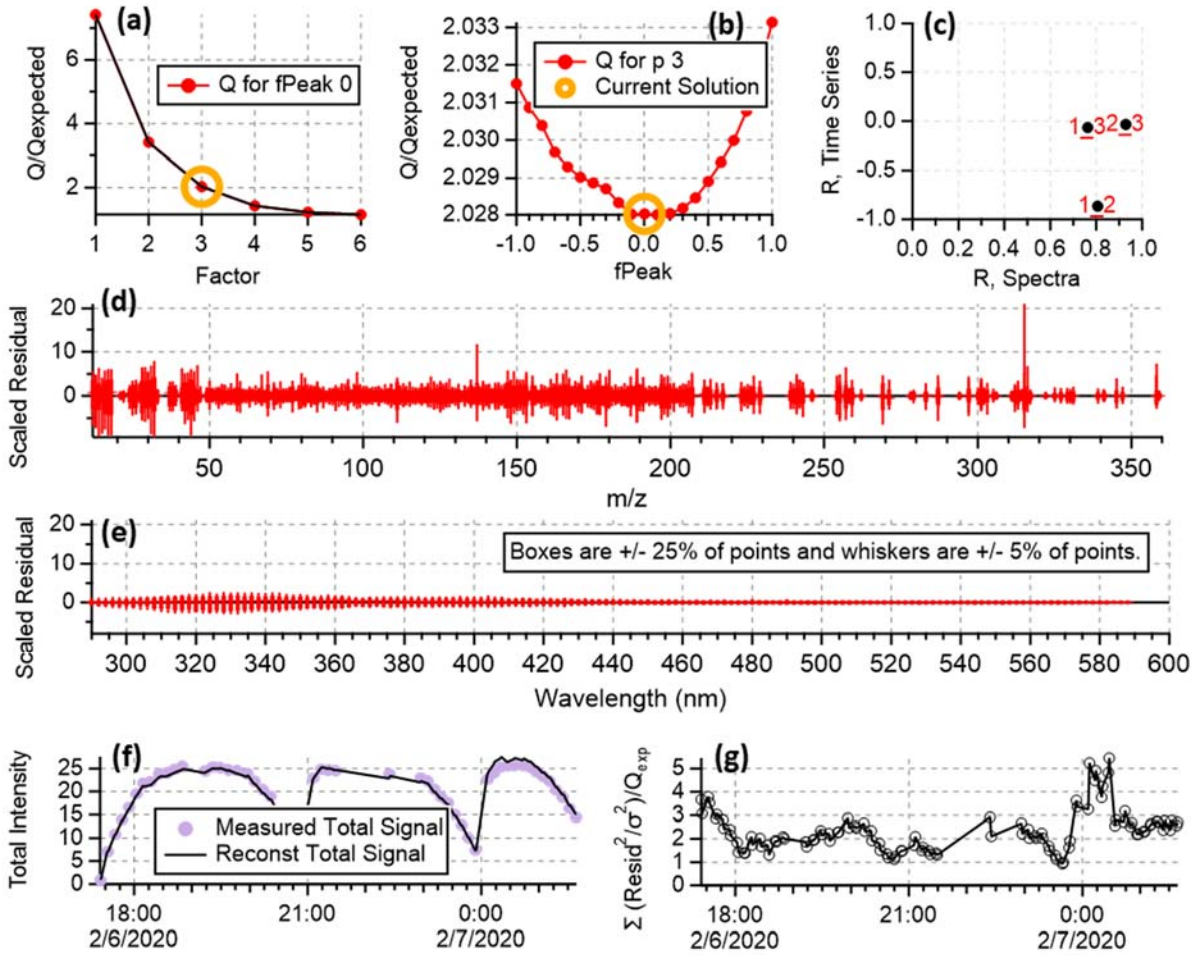

Figure S2. Summary of diagnostic plots of the PMF analysis of the ^{3}C*-initiated reactions: (a) Q/Qexp as a function of number of factors selected for PMF modeling. (b) Q/Qexp as a function of fPeak. (c) Correlations among PMF factors. (d) Box and whisker plot showing the distributions of scaled residuals for each AMS ion. (e) Box and whisker plot showing the distributions of scaled residuals for each light absorption wavelength. (f) Reconstructed and measured total signal for each sample. (g) Q/Qexp for each sample.

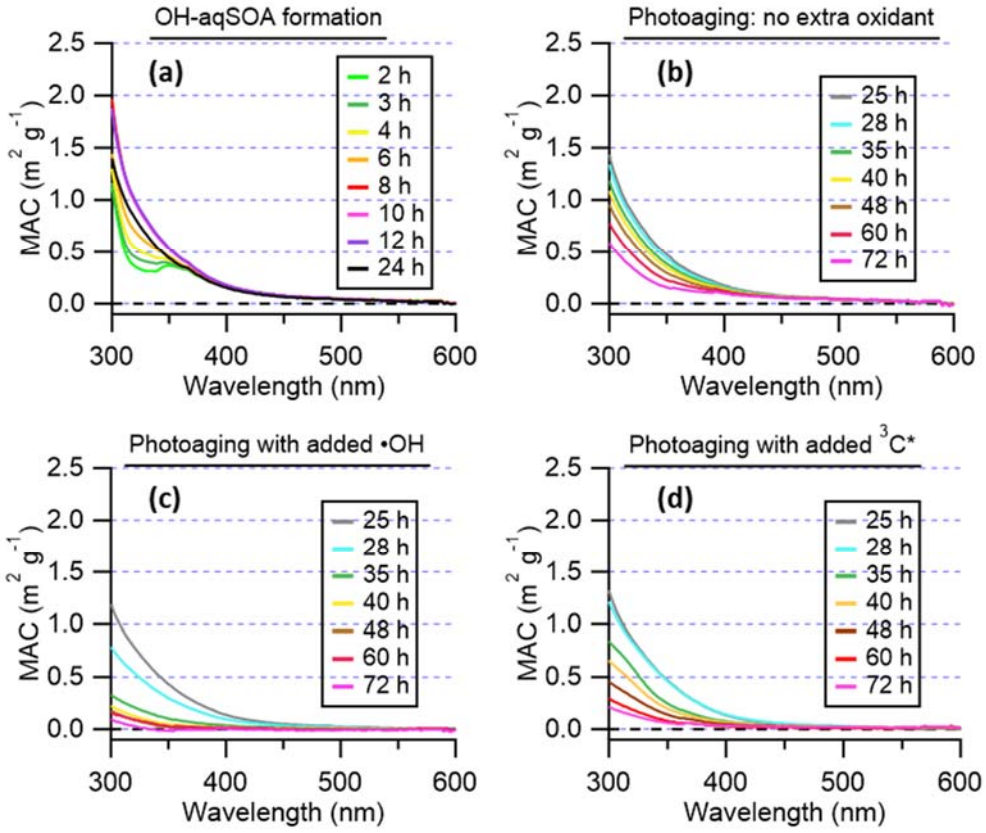

Figure S3. Evolution of the mass absorption coefficient spectra of the GA •OH-aqSOA.

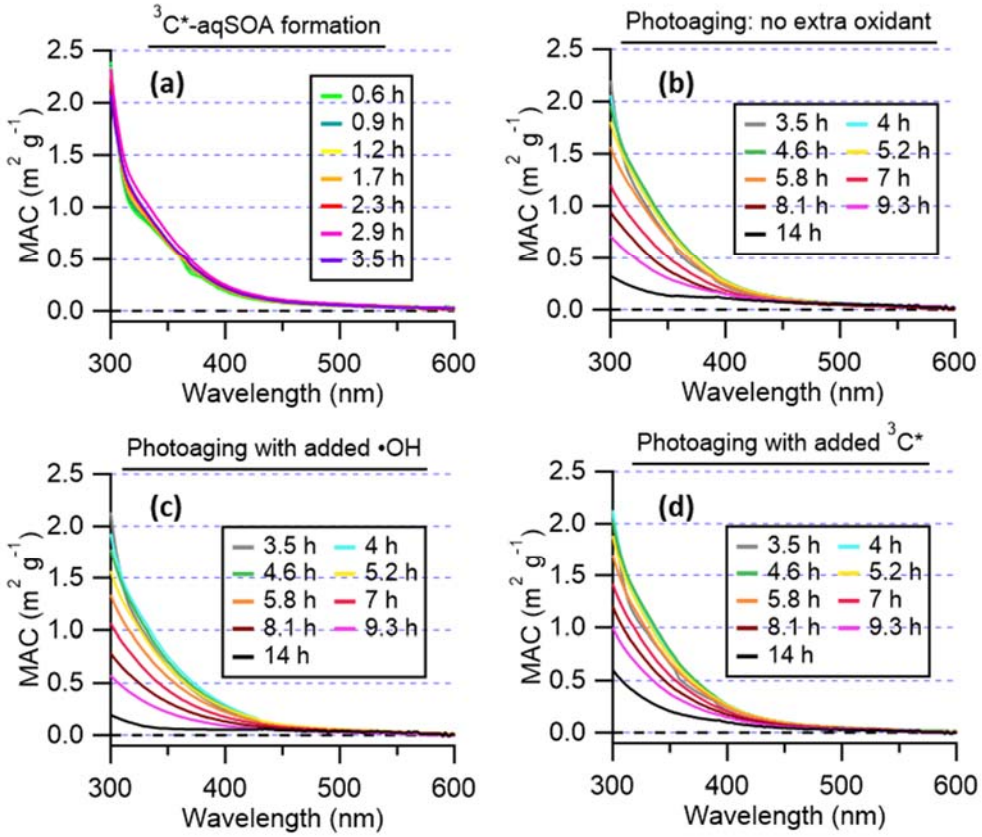

Figure S4. Evolution of the mass absorption coefficient spectra of the GA ^{3}C*-aqSOA.

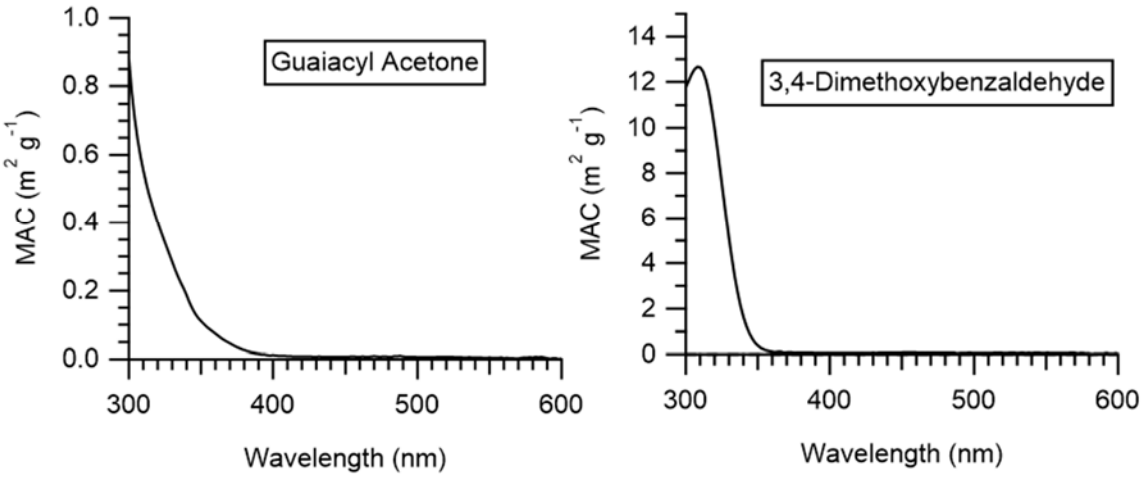

Figure S5. Mass absorption coefficient spectra of guaiacyl acetone and 3,4-dimethoxybenzaldehyde.

90

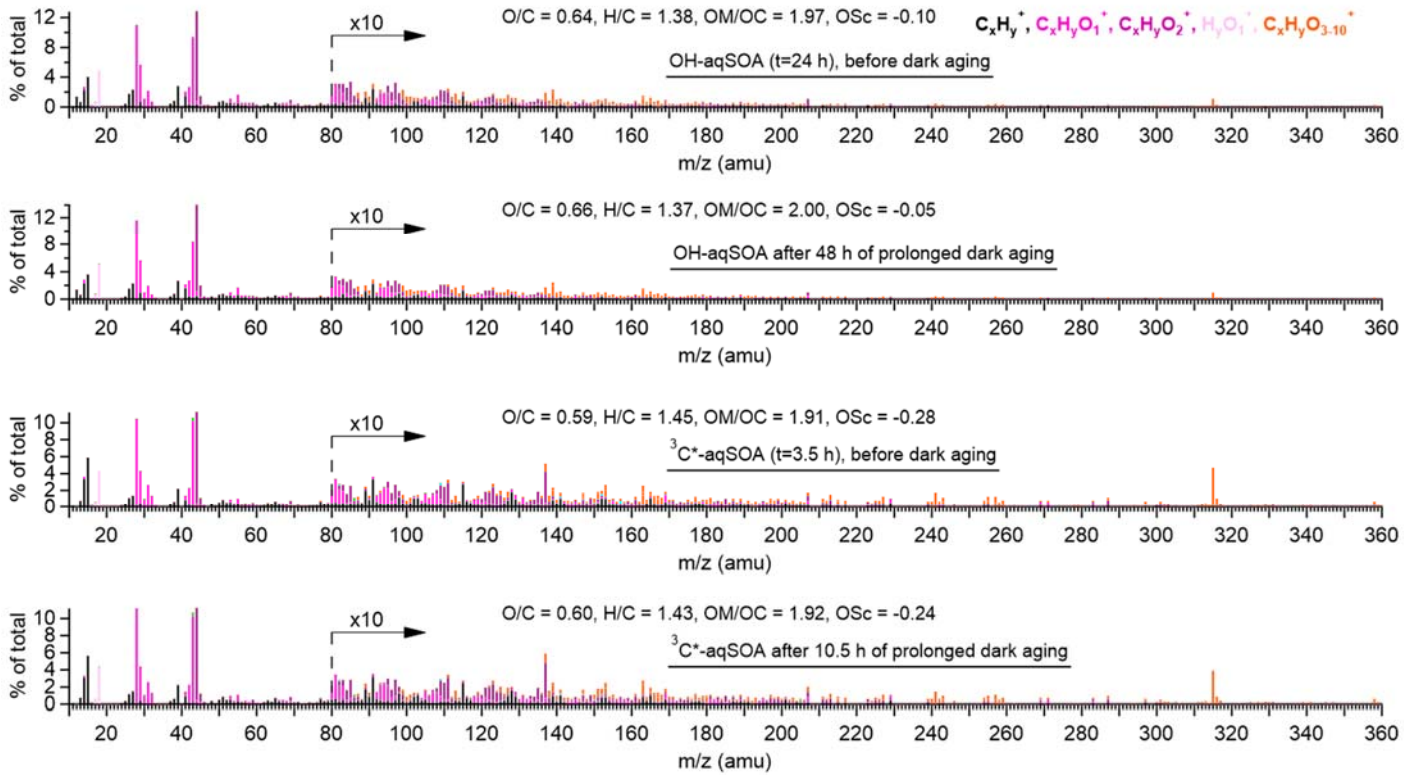

Figure S6. AMS spectra of the •OH-aqSOA and ^{3}C*-aqSOA before and after aging in the dark.

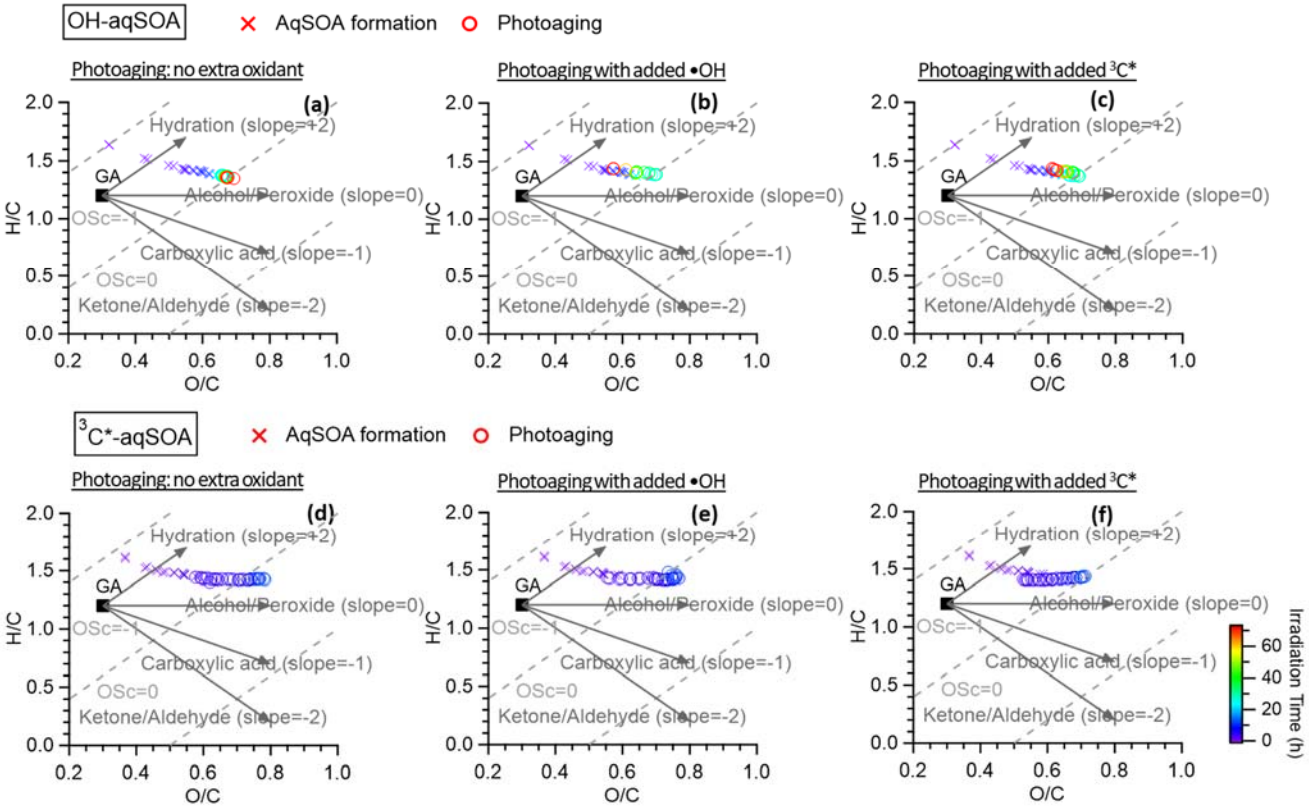

Figure S7. Van Krevelen diagrams that illustrate the evolution trends of the •OH-aqSOA and $^{3}C^{*}$-aqSOA under different photoaging conditions.

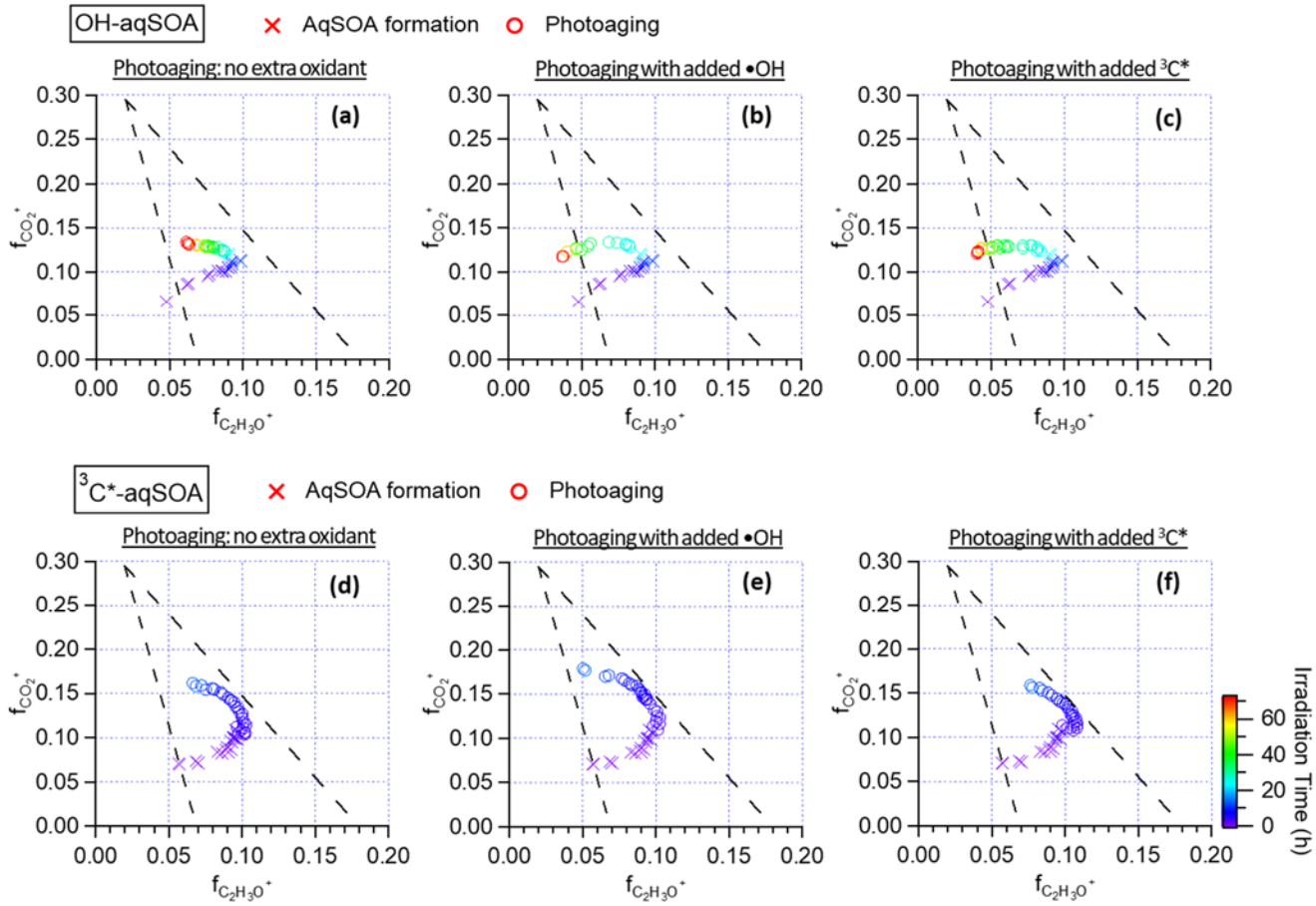

Figure S8. Triangle plots (f_{CO2+} vs f_{C2H3O+}) that depict the evolution trends of the •OH-aqSOA and ^{3}C*-aqSOA under different photoaging conditions.

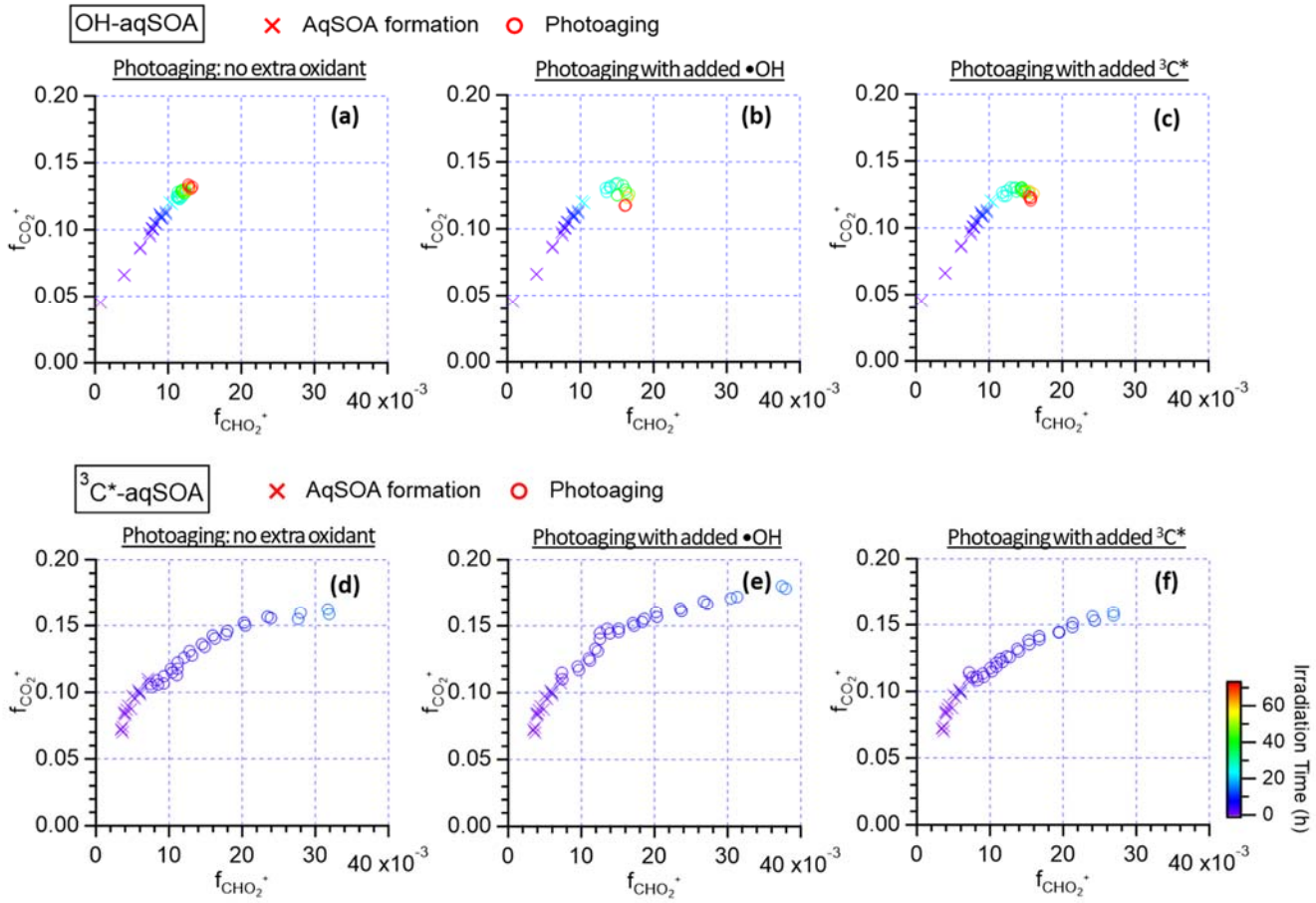

Figure S9. The plots of f_{CO2+} vs f_{CHO2+} that depict the carboxylic acid formation in the •OH-aqSOA and the ^{3}C*-aqSOA under different photoaging conditions.

105

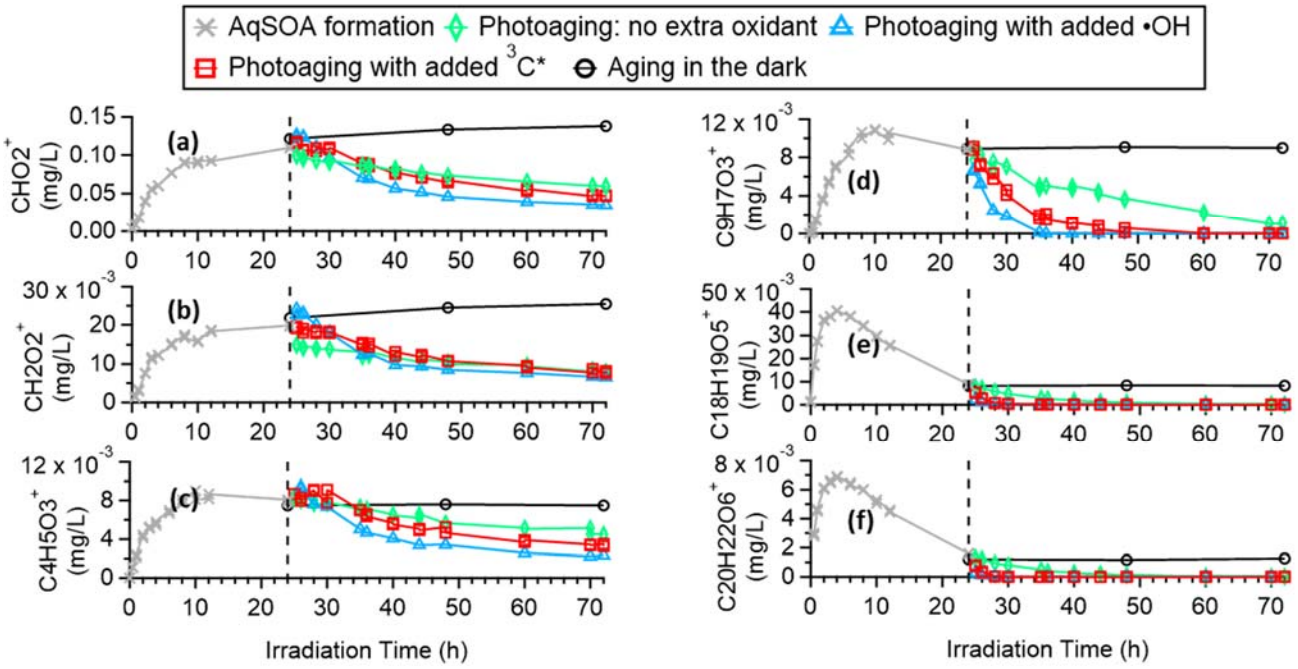

Figure S10. Time trend of selected AMS tracer ions in the •OH-aqSOA during aqSOA formation and prolonged aging.

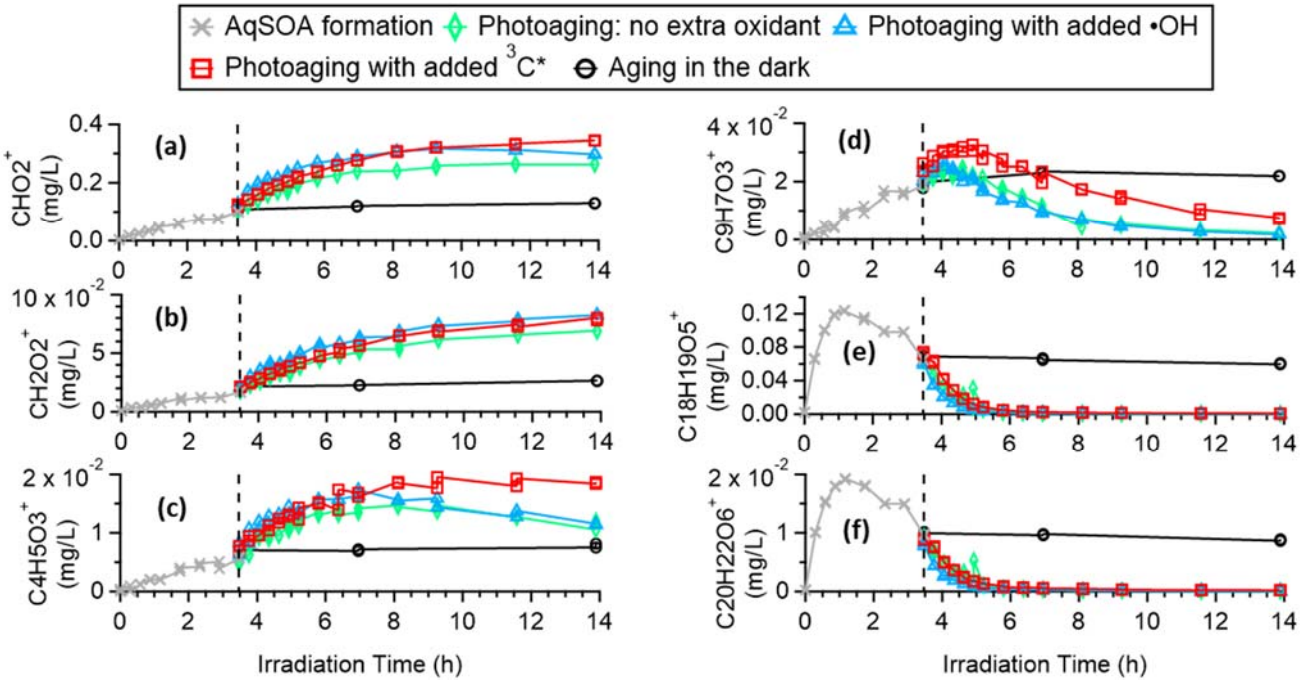

Figure S11. Time trends of selected AMS tracer ions in the $^{3}C^{*}$-aqSOA during aqSOA formation and prolonged aging.

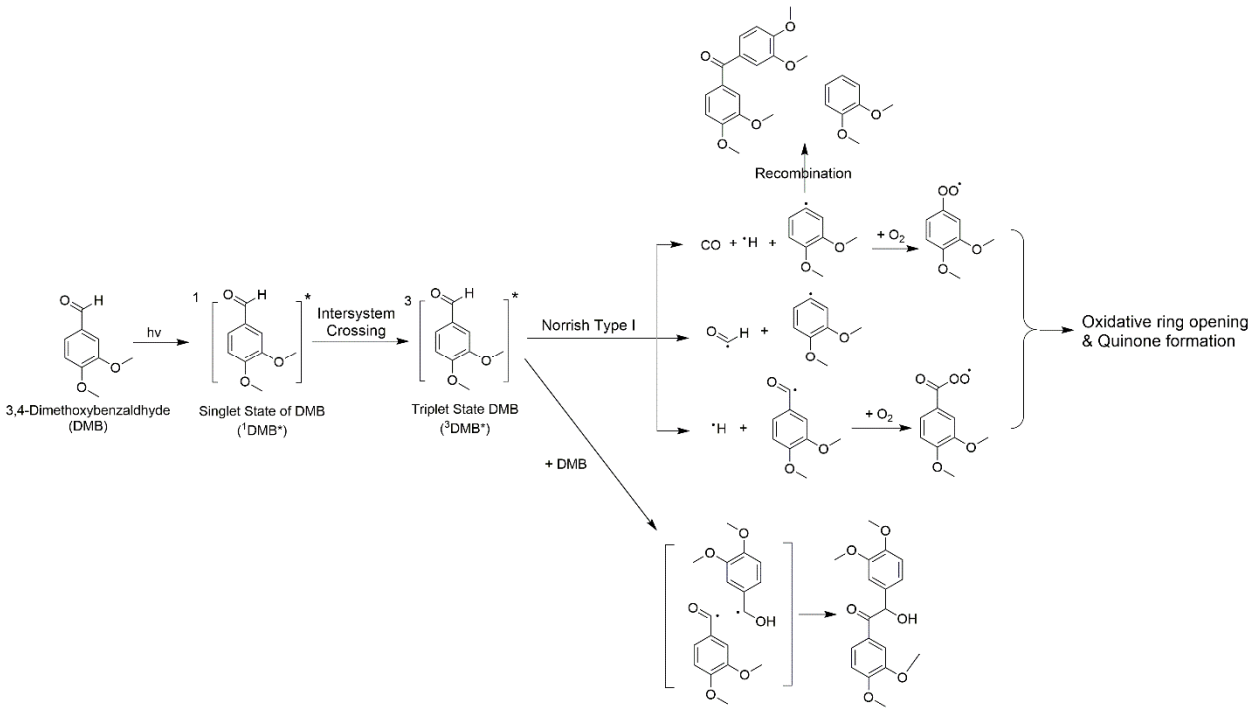

Scheme S1. Postulated reaction pathways for the photodegradation of 3,4-dimethoxybenzaldehyde. The mechanisms are adapted from previous studies on benzaldehydes (Berger et al., 1973; Dubtsov et al., 2006; Shen and Fang, 2011; Theodoropoulou et al., 2020).

Reference

Berger, M., Goldblatt, I. L. and Steel, C.: Photochemistry of benzaldehyde, J. Am. Chem. Soc., 95(6), 1717–1725, doi:10.1021/ja00787a004, 1973.

Dubtsov, S. N., Dultseva, G. G., Dultsev, E. N. and Skubnevskaya, G. I.: Investigation of Aerosol Formation During Benzaldehyde Photolysis, J. Phys. Chem. B, 110(1), 645–649, doi:10.1021/jp0555394, 2006.

Shen, L. and Fang, W.-H.: The Reactivity of the 1,4-Biradical Formed by Norrish Type Reactions of Aqueous Valerophenone: A QM/MM-Based FEP Study, J. Org. Chem., 76(3), 773–779, doi:10.1021/jo101785z, 2011.

Theodoropoulou, M. A., Nikitas, N. F. and Kokotos, C. G.: Aldehydes as powerful initiators for photochemical transformations, Beilstein J. Org. Chem., 16, 833–857, 2020.